*Optica Applicata, Vol. XXXVII, No. 3, 2007*

# Design of athermal arrayed waveguide grating using silica/polymer hybrid materials

DE-LU LI, CHUN-SHENG MA*, ZHENG-KUN QIN, HAI-MING ZHANG, DA-MING ZHANG, SHI-YONG LIU

State Key Laboratory on Integrated Optoelectronics, College of Electronic Science and Engineering, Jilin University, Changchun 130012, China

*Corresponding author: mcsheng@163.com

This study demonstrates a novel athermal arrayed waveguide grating (AWG) which is composed of silica/polymer hybrid materials on a silicon substrate. The temperature-dependent wavelength shift of the AWG depends on the refractive indices of the materials and the size of the waveguide. The athermalization of the AWG can be realized by selecting the proper values of the material and structural parameters of the device.

Keywords: arrayed waveguide grating, temperature-dependent wavelength shift, athermalization.

## 1. Introduction

Because of their excellent features and potential applications, the arrayed waveguide gratings (AWG) have currently received considerable attention and have become key components in dense wavelength-division-multiplexing (DWDM) networks [1–4]. However, an AWG made of silica is very sensitive to temperature. Therefore, in order to realize the normal operation of the AWG, the temperature control unit is required, *i.e.*, a heater or a Peltier cooler. To eliminate the undesirable temperature dependence, the athermalization should be realized in the operation of the AWG devices [5–10]. An excellent athermal AWG enables the performance of the AWG unaffected by ambient temperature variation.

Recently, a hybrid waveguide with a silica core and polymer overcladding is considered as the most attractive athermal structure because of its resistance to the thermo-optic sensitivity of the materials and its simple fabrication process [11].

In this study, such an athermal AWG is designed by theoretic simulation. First, the principle of the athermal AWG with silica/polymer hybrid materials is described, and the relative formulas are derived for analyzing the temperature dependence of the AWG. Then, the theoretical simulation and optimum design of the athermal

AWG are carried out. Finally, a conclusion is reached, based on the analysis and the discussion.

## 2. Principle of athermal AWG

In this section, we present the athermal condition and the relative formulas of silica/polymer hybrid material AWG on a silicon substrate. The temperature/wavelength tuning rate $\mathrm{d}\lambda_c/\mathrm{d}T$ of the AWG is expressed as [12]

$$\frac{\mathrm{d}\lambda_c}{\mathrm{d}T} = \frac{\lambda_c}{n_c}\left(\frac{\mathrm{d}n_c}{\mathrm{d}T} + n_c\alpha_{\mathrm{sub}}\right) \tag{1}$$

where $T$ is the temperature; $\lambda_c$ is the center wavelength in free-space; $n_c$ is the mode effective refractive index which is defined as $n_c = (\lambda_c/2\pi)k_z$, here $k_z$ is the mode propagation constant along the propagating direction $z$; $\mathrm{d}n_c/\mathrm{d}T$ is the thermo-optic (TO) coefficient of the waveguide; and $\alpha_{\mathrm{sub}}$ is the coefficient of thermal expansion (CTE) of the substrate. Integrating Eq. (1), we can obtain

$$\lambda_c = Cn_c\exp(\alpha_{\mathrm{sub}}T) \tag{2}$$

where $C$ is an integrating coefficient. Assume that $\lambda_c = \lambda_0$ and $n_c = n_{c0}$ when $T = T_0$, then we can determine $C$ as

$$C = \frac{\lambda_0}{n_{c0}}\exp(-\alpha_{\mathrm{sub}}T_0) \tag{3}$$

Substituting Eq. (3) into Eq. (2), we get

$$\lambda_c = \frac{\lambda_0 n_c}{n_{c0}}\exp\left[\alpha_{\mathrm{sub}}(T - T_0)\right] \tag{4}$$

Thus, from Eq. (4) we obtain the central wavelength shift caused by the temperature variation as

$$\Delta\lambda = \lambda_c - \lambda_0 = \frac{\lambda_0}{n_{c0}}\left\{n_c\exp\left[\alpha_{\mathrm{sub}}(T - T_0)\right] - n_{c0}\right\} \tag{5}$$

Taking $\Delta\lambda = 0$, from Eq. (5) we can obtain the athermal condition of the AWG as

$$\alpha_{\mathrm{sub}}(T - T_0) = \ln\left(\frac{n_{c0}}{n_c}\right) \tag{6}$$

By differentiating Eq. (6), the athermal condition of the AWG can also be expressed in another form as follows

$$n_c \alpha_{\text{sub}} = -\frac{\mathrm{d}n_c}{\mathrm{d}T} \tag{7}$$

Because the effective refractive index $n_c$ is dependent on the refractive indices of the materials and on the size and the shape of the waveguide, then by selecting proper material and structural parameters of the waveguide to satisfy Eq. (6) or (7), an athermal AWG can be designed.

## 3. Simulation and design of athermal AWG

In this section, we carry on the theoretical simulation and the optimum design of an athermal AWG with silica/polymer hybrid materials.

Figure 1**a** shows the scheme of an AWG device which consists of two focusing slab waveguides, $2N+1$ input/output channels, and $2M+1$ arrayed waveguides. The core cross-sections of the input/output channels and the arrayed waveguides are designed as rectangles with the core width $a$ and the core thickness $b$. Figure 1**b** shows the cross-section and the refractive index profile of the input/output channels and the arrayed waveguides. We design three layer hybrid waveguide structure which contains a silica substrate of a 500 μm thickenss, a silica undercladding of a 15 μm thickness and with the refractive index $n_2 = 1.445$ [12], a silica core of the core size $a = b = 5$ μm (in width and in thickness) and with the refractive index $n_1 = 1.454$ [12], and a polymer overcladding of a 15 μm thicknenss and with the refractive index $n_3 = 1.440$ [12]. Assume that both the silica undercladding and the silica core have the same positive material TO coefficient, that is $\mathrm{d}n_1/\mathrm{d}T = \mathrm{d}n_2/\mathrm{d}T = 1.0\times10^{-5}$ /°C [13].

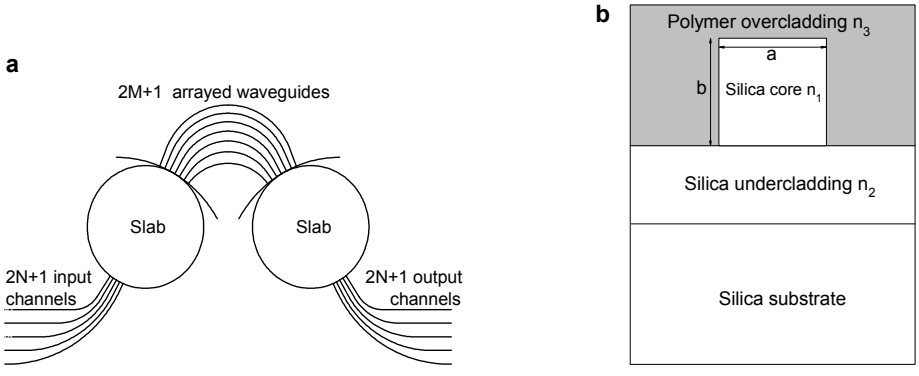


Fig. 1. Scheme of an AWG (**a**), and cross-section and refractive index profile (**b**) of the input/output channels and the arrayed waveguides.

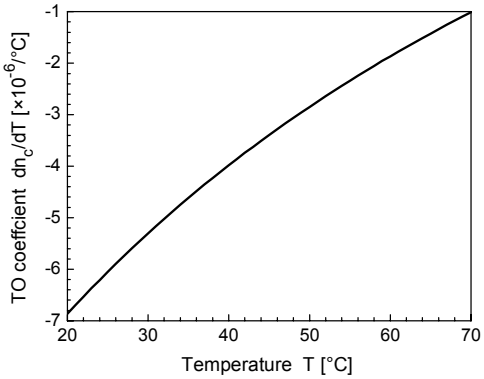


Fig. 2. Dependence of TO coefficient $dn_c/dT$ on temperature $T$, where $n_1 = 1.454$, $n_2 = 1.445$, $n_3 = 1.440$, $a = b = 5.0$ μm, $dn_1/dT = dn_2/dT = 1.0\times10^{-5}$ /°C, and $dn_3/dT = -1.1\times10^{-4}$ /°C.

To reduce the temperature dependence of the wavelength shift, the polymer overcladding has a negative material TO coefficient of $dn_3/dT = -1.1\times10^{-4}$ /°C [13]. The center wavelength at temperature $T_0$ is selected to be $\lambda_0 = 1550.918$ nm (or 193.3 THz for frequency), which is one of the standard wavelengths recommended by the International Telecommunications Union (ITU) [14]. This AWG device is made on the silicon substrate, having a CTE of $\alpha_{sub} = 2.63\times10^{-6}$ /°C [13].

Because the environmental temperature of an AWG is usually changed from 20 °C to 70 °C, we only discuss the central wavelength shift $\Delta\lambda$ in this range of temperature variation. The subsequent relations between the wavelength shift $\Delta\lambda$ and the refractive indices of the core, undercladding and overcladding $n_1$, $n_2$, $n_3$ (as well as the core width and core thickness $a$, $b$) are analyzed and discussed as follows.

First, it is necessary to investigate the behavior of the TO coefficient $dn_c/dT$ of the waveguide. The values of $dn_c/dT$ at different values of temperatures can be determined by using the finite difference method. The TO coefficient $dn_c/dT$ can be approximately expressed as

$$\frac{dn_c}{dT} \approx \frac{\Delta n_c}{\Delta T} \tag{8}$$

where $\Delta n_c = n_{c2} - n_{c1}$, $\Delta T = T_2 - T_1$, $n_c = n_{c1}$ and $n_c = n_{c2}$ when $T = T_1$ and $T = T_2$, respectively, and $T_1$ and $T_2$ are very close to each other, then $\Delta n_c$ and $\Delta T$ are very small quantities.

Figure 2 shows the dependence of the TO coefficient $dn_c/dT$ on the temperature $T$. We can find that $dn_c/dT$ is not constant with the variation of the temperature which nonlinearly increases as the temperature increases, although $dn_1/dT$, $dn_2/dT$ and $dn_3/dT$ are constants, respectively. Therefore, this behavior of $dn_c/dT$ will obviously affect the shifts of the central wavelength and the transmission spectrum of the AWG caused by the variation of the temperature.

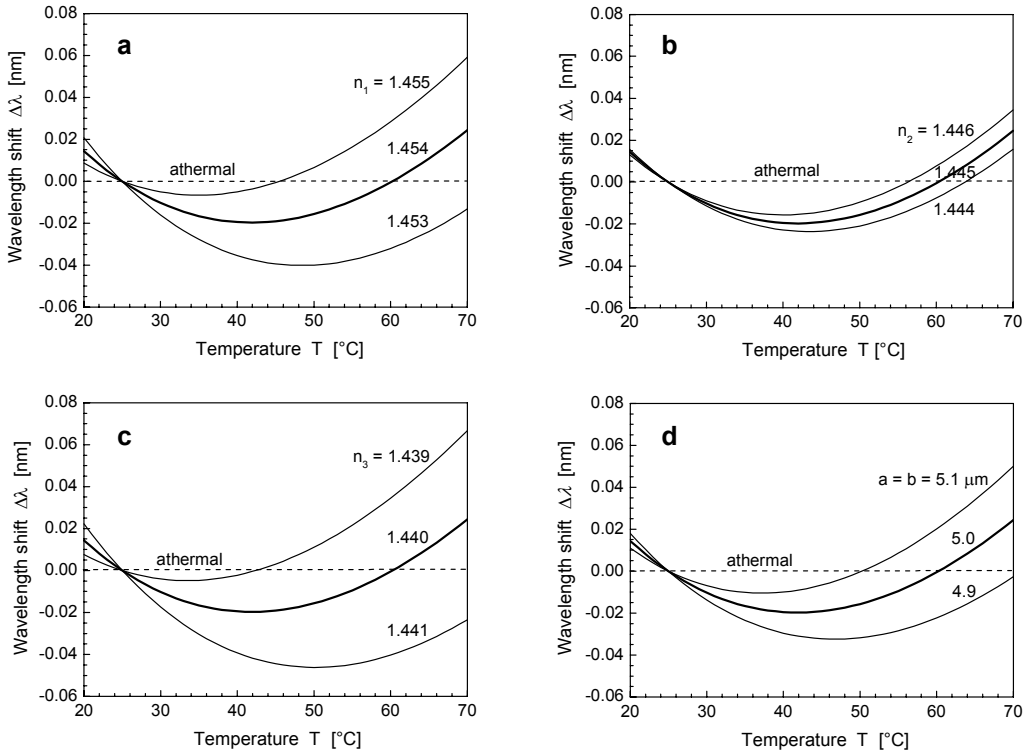


Fig. 3. Dependence of central wavelength shift $\Delta\lambda$ on refractive indices $n_1$, $n_2$, $n_3$ and core width $a$ and core thickness $b$ for the designed athermal hybrid material AWG, where $dn_1/dT = dn_2/dT = 1.0\times10^{-5}$ /°C, $dn_3/dT = -1.1\times10^{-4}$ /°C; $n_2 = 1.445$, $n_3 = 1.440$, and $a = b = 5.0$ μm, and $n_1 = 1.453$, 1.454, 1.455 (**a**); $n_1 = 1.454$, $n_3 = 1.440$, $a = b = 5.0$ μm, and $n_2 = 1.444$, 1.445, 1.446 (**b**); $n_1 = 1.454$, $n_2 = 1.445$, $a = b = 5.0$ μm, and $n_3 = 1.439$, 1.440,1.441 (**c**); $n_1 = 1.454$, $n_2 = 1.445$, $n_3 = 1.440$, and $a = b = 4.9$, 5.0, 5.1 μm (**d**).

Figure 3 shows the dependences of the central wavelength shift $\Delta\lambda$ on the refractive indices of the core, undercladding and overcladding $n_1$, $n_2$, $n_3$ as well as the core width and core thickness $a$ and $b$ for the designed athermal hybrid material AWG, which are calculated from Eq. (5). We can see that there exists an optimal operation condition of the AWG, which should guarantee the central wavelength shift to be small enough in a sufficiently large range of the temperature variation. To be precise, when we select $n_1 = 1.454$, $n_2 = 1.445$, $n_3 = 1.440$ and $a = b = 5$ μm (the thick line in every sub-figure), the central wavelength shift is within the range of $-0.020 \sim 0.022$ nm as the temperature increases from 0 °C to 70 °C. In this case we can presume that the athermalization is realized in the designed AWG.

Figure 4 compares the central wavelength shift $\Delta\lambda$ of the conventional silica AWG with the designed athermal hybrid material AWG, which are calculated from Eq. (5). The refractive index and the TO coefficient of the silica overcladding of

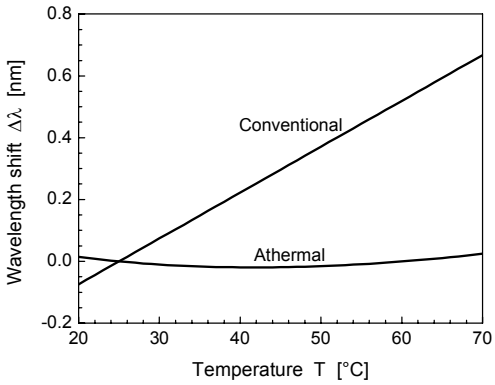


Fig. 4. Comparison of central wavelength shift $\Delta\lambda$ of the conventional silica AWG with the designed athermal hybrid material structure AWG, where $dn_1/dT = dn_2/dT = 1.0\times10^{-5}$ /°C, $a = b = 5.0$ μm, $n_1 = 1.454$, $n_2 = 1.445$, $n_3 = 1.440$, and $dn_3/dT = 1.0\times10^{-5}$ /°C (for conventional AWG) and $-1.1\times10^{-4}$ /°C (for designed athermal AWG).

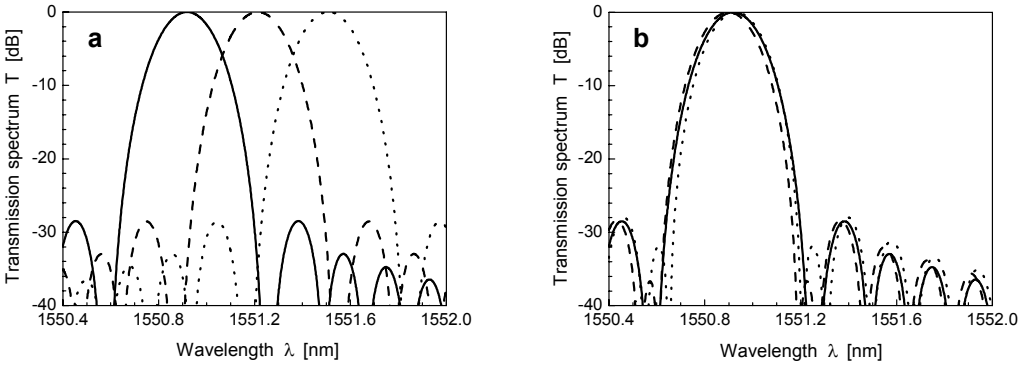


Fig. 5. Comparison of transmission spectrum of the conventional silica AWG with the designed athermal hybrid material AWG, where $dn_1/dT = dn_2/dT = 1.0\times10^{-5}$ /°C, $a = b = 5.0$ μm, $n_1 = 1.454$, $n_2 = 1.445$, $n_3 = 1.440$, $T = 25$ °C (solid line), 45 °C (dashed line), 65 °C (dotted line): $dn_3/dT = 1.0\times10^{-5}$ /°C (for conventional AWG) – **a**, and $dn_3/dT = -1.1\times10^{-4}$ /°C (for designed athermal AWG) – **b**.

the conventional silica AWG are taken to be $n_3 = 1.440$ and $dn_3/dT = 1.0\times10^{-5}$ /°C, respectively. We can observe that as the temperature increases from 20 °C to 70 °C, the central wavelength shift of the conventional silica AWG increases to 0.66 nm, while that of the designed athermal hybrid material AWG only increases to 0.025 nm. This indicates that the central wavelength shift of the designed athermal hybrid material AWG is much lower than that of the conventional silica AWG.

Figure 5 compares the transmission spectrum of the conventional silica AWG with the designed athermal hybrid material AWG, which are calculated from Eq. (4) in [15], the temperature $T = 25$ °C, 45 °C, 65 °C. The refractive index and the TO coefficient of the silica overcladding of the conventional silica AWG are taken to be

$n_3 = 1.440$ and $dn_3/dT = 1.0\times10^{-5}$ /°C. We can see that the transmission spectrum shift of the conventional silica AWG is about 0.30 and 0.60 nm, while that of the designed athermal hybrid material AWG is only about –0.019 and 0.011 nm, as the temperature increases from 25 °C to 45 °C and 65 °C. This indicates that the transmission spectrum shift of the designed athermal hybrid material AWG is much lower than that of the conventional silica AWG.

## 4. Conclusions

After the preceding analysis and discussion about the athermal hybrid material AWG, a conclusion is reached as follows.

In this paper, we present a novel technique for theoretical simulation and optimum design of the athermal AWG with silica/polymer hybrid materials. By selecting the proper values of the refractive indices of the materials and the size of the waveguide, the athermalization can be realized in the silica/polymer hybrid material AWG. To be precise, the center wavelength shift of the designed athermal hybrid material AWG only increases to 0.025 nm, while that of the conventional silica AWG increases to 0.66 nm, as the temperature increases from 20 °C to 70 °C. The transmission spectrum shift of the designed athermal hybrid material AWG is only about –0.019 and 0.011 nm, while that of the conventional silica AWG is about 0.30 and 0.60 nm, as the temperature increases from 25 °C to 45 °C and 65 °C.

This work, we think, is not only valid for the presented AWGs, but also helpful for other optical devices based on hybrid material waveguides to realize the athermalization.

*Acknowledgments* – The authors wish to express their gratitude to the National Science Foundation Council of China (the project no. 60576045) for its generous support to this work.

### References

[1] STARING A.A.M., SMIT M.K., *Phased-array-based photonic integrated circuits for wavelength division multiplexing applications*, IEICE Transactions on Electronics **E80-C**(5), 1997, pp. 646–53.

[2] ROBITAILLE L., CALLENDER C.L., NOAD J.P., *Polymer waveguide devices for WDM applications*, Proceedings of the SPIE **3281**, 1998, pp. 14–24.

[3] KOTELES E.S., *Integrated planar waveguide demultiplexers for high-density WDM applications*, Fiber and Integrated Optics **18**(4),1999, pp. 211–44.

[4] HIROTA H., ITOH M., OGUMA M., HIBINO Y., *Athermal arrayed-waveguide grating multi/demultiplexers composed of $TiO_2$-$SiO_2$ waveguides on Si*, IEEE Photonics Technology Letters **17**(2), 2005, pp. 375–77.

[5] INOUE Y., KANEKO A., HANAWA F., TAKAHASHI H., HATTORI K., SUMIDA S., *Athermal silica-based arrayed-waveguide grating multiplexer*, Electronics Letters **33**(23), 1997, pp. 1945–7.

[6] KANEKO A., KAMEI S., INOUE Y., TAKAHASHI H., SUGITA A., *Athermal silica-based arrayed -waveguide grating (AWG) multi/demultiplexer with new low loss groove design*, Electronics Letters **36**(4), 2000, pp. 318–9.

[7] TANOBE H., KONDO Y., KADOTA Y., OKAMOTO K., YOSHIKUNI Y., *Temperature insensitive arrayed waveguide gratings on InP substrates*, IEEE Photonics Technology Letters **10**(2), 1998, pp. 235–7.

[8] KEIL N., YAO H.H., ZAWADZKI C., BAUER J., BAUER M., DREYER C., SCHNEIDER J., *Athermal all-polymer arrayed-waveguide grating multiplexer*, Electronics Letters **37**(9), 2001, pp. 579–80.
[9] OOBA N., HIBINO Y., INOUE Y., SUGITA A., *Athermal silica-based arrayed-waveguide grating multiplexer using bimetal plate temperature compensator*, Electronics Letters **36**(21), 2000, pp. 1800–1.
[10] MARU K., OHKAWA M., NOUNEN H., TAKASUGI S., KASHIMURA S., OKANO H., UETSUKA H., *Athermal and center wavelength adjustable arrayed-waveguide grating*, Optical Fiber Communication Conference, Technical Digest, Vol. 2, 2000, pp. 130–2.
[11] KOKUBUN Y., FUNATO N., TAKIZAWA M., *Athermal waveguide for temperature-independent lightwave devices*, IEEE Photonics Technology Letters **5**(11), 1993, pp. 1297–300.
[12] ZHU D.Q., XU Z., LU D.S., *An athermal AWG with hybrid material structure waveguide*, Proceedings of the SPIE **4904**, 2002, pp. 485–9.
[13] KEIL N., YAO H.H., ZAWADZKI C., *Athermal polarization-independent arrayed waveguide grating (AWG) multiplexer using an all-polymer approach*, Applied Physics B: Lasers and Optics **73**(5–6), 2001, pp. 619–22.
[14] KUZNETSOV M., FROBERG N.M., HENLON S.R., REINKE C., FENNELLY C., *Dispersion-induced power penalty in fiber-Bragg-grating WDM filter cascades using optically preamplified and nonpreamplified receivers*, IEEE Photonics Technology Letters **12**(10), 2000, pp. 1406–8.
[15] MA C.S., WANG X.Y., ZHANG H.M., ZHANG D.-M., CUI Z.C., LIU S.Y., *An efficient technique for analyzing transmission characteristics of arrayed waveguide grating multiplexers*, Optical and Quantum Electronics **36**(8), 2004, pp. 759–71.

*Received May 10, 2007*
*in revised form July 31, 2007*